A Numerical Investigation of All-Analog Radio Self-Interference Cancellation

Armen Gholian, Yiming Ma, Yingbo Hua, *Fellow, IEEE*
Department of Electrical Engineering, University of California, Riverside, CA, USA

***Abstract*—Radio self-interference cancellation (SIC) is the fundamental enabler for full-duplex radios. While SIC methods based on baseband digital signal processing and/or beamforming are inadequate, an all-analog method is useful to drastically reduce the self-interference as the first stage of SIC. However, all-analog radio SIC has so far received very little academic attention in terms of its architectural design and performance limit. In this paper, we present such an early effort. We show that a recently used uniform architecture with uniformly distributed RF attenuators has a performance highly dependent on the carrier frequency. We also show that a new architecture with the attenuators distributed in a clustered fashion has important advantages over the uniform architecture. These advantages are shown numerically through random multipath interference channels, number of control bits in step attenuators, attenuation-dependent phases, single and multi-level structures, etc. These insights will be useful in guiding future hardware-based experiments.**

***Index Terms*—interference cancellation, full-duplex radio, all-analog cancellation**

I. Introduction

The wireless communication devices currently employed are all half-duplex and use either a frequency-division or time-division approach to transmit and receive. A more spectrally efficient approach, *full-duplex*, has received growing interest in the research community. The main challenge in full-duplex is that the transmitted signal created by the device's own transmitter, known as *self-interference*, is very strong at the device's own receiver. Only by canceling self-interference to the noise floor, could full-duplex be realizable and the throughput be doubled.

As shown in [1], the methods for SIC can be grouped as *all-analog* [2]–[6], *all-digital* [7] and *hybrid* [1], [8]–[10]. In an all-analog method, RF interference is canceled at RF frontend by using its RF interference source. In an all-digital method, interference is canceled only after the RF interference has been converted into baseband and digitized. A hybrid method may use either a baseband-controlled transmit beamforming method to cancel interference at the RF frontend of receivers [10] or use the RF signals tapped from the output of RF power amplifiers to cancel the interference after down-conversion to a lower frequency [1].

In general, a combination of these methods is required to fully realize full-duplex, but an all-analog cancellation is necessary in most situations. This is because (1) an all-analog cancellation can leave no or little additional noise in the residual self-interference, and (2) its performance in principle is not limited by the transmitter noise or by the transmitter nonlinearity. The most successful result was shown in [5], which uses an analog filter with uniformly distributed RF attenuators. This uniform architecture is also used in [6].

In this paper, we propose a novel architecture for all-analog cancellation called *clustered* architecture and compare its performance with the *uniform* architecture, used in [5], [6]. We evaluate the statistical limits of each architecture through simulation and investigate the impact of imperfections of attenuators on the performance of the canceler. Furthermore, unlike previous works, we consider a wide range of realizations of a random interference channel model. We show how the cancellation performance in each architecture varies with the changes in the number of taps, and the relative delay between two adjacent taps of the canceler; environmental path loss; and the number of control bits, and the phase of the attenuators. We also investigate the impact of random perturbations to the uniform architecture. Finally, we investigate the impact of multi-level cancellation in each architecture.

The rest of this paper is organized as follows: the cancellation channel models of the uniform and clustered architectures are presented in Section II; tuning algorithms for ideal and non-ideal attenuators are given in Section III; expressions for performance evaluation are defined in Section IV; simulation results are presented in Section V; and the paper is concluded in Section VI.

II. Cancellation Channel Model

In Fig. 1(a), structure of a general all-analog canceler is shown. The goal in an all-analog canceler is to mimic the interference channel so that the output signal of all-analog canceler be well-matched to self-interference signal and consequently the residual interference be as small as possible. The matching can be done either in the frequency domain or in the time domain. Similar to [4], [5], our approach is in the frequency domain.

The frequency response of a RF multipath interference channel $H(\omega)$ (before being converted to baseband) is

$$H(\omega) = \sum_{i=0}^{I-1} a_i e^{-j\omega\tau_i} \tag{1}$$

where $a_i > 0$ is the attenuatuin of the ith path, τ_i is the delay of the ith path, and I is the number of multipath components, where I, a_i, and τ_i are all unknown. The goal is to come up with a model that *approximates* the wireless multipath channel (1) well and is also easily *implementable* (particularly, no use of variable delays in the architecture).

This work was supported in part by ARO under Contract No. W911NF1210432 and UCOP under Grant No. PC-12-247260.

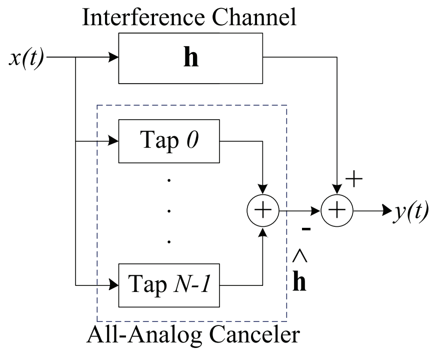

(a) System model for all-analog radio SIC

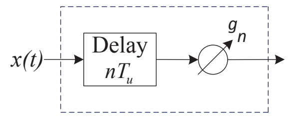

(b) nth tap of the uniform canceler, $n = 0, 1, ..., N-1$

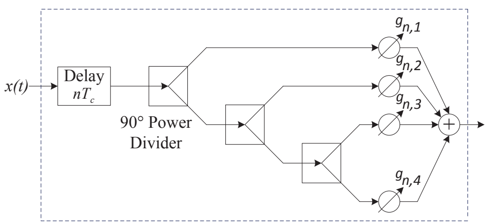

(c) nth c-tap of the clustered canceler, $n = 0, 1, ..., N-1$

Fig. 1. (a) System model for all-analog radio SIC, (b) architecture of each tap of the uniform canceler, and (c) arcitecture of each tap of the clustered canceler. $x(t)$ is the transmitted signal and $y(t)$ is the residual interference.

One such a model is the uniform structure, used in [5], [6]. The structure of each tap of the uniform canceler is shown in Fig. 1(b) where each tap consists of one adjustable attenuator and a fixed time delay. Therefore, based on Fig. 1(a) and 1(b), the frequency response of the uniform canceler is

$$\hat{H}_{\mathrm{u}}(\omega) = e^{-j\omega T_0} \sum_{n=0}^{N-1} g_n e^{-j\omega n T} \tag{2}$$

where T_0 is the delay of the zero-th tap (not shown in the figure), N is the number of taps, and T is the relative delay between two adjacent taps. Although the uniform canceler provides a good performance [5], it is sensitive to the carrier frequency, as will be shown later.

In this paper, we propose a clustered architecture where the RF attenuators are distributed in clusters. The structure of each tap of the clustered canceler, known as clustered-tap or *c-tap*, is shown in Fig. 1(c). Each c-tap is a cluster of four adjustable attenuators connected together via three cascaded 90° power dividers, and an RF cable for fixed time delay. A 90° power divider, splits an RF signal into two which differ from each other by 90° in phase. Based on Fig. 1(a) and 1(c), frequency response of the clustered canceler is

$$\hat{H}_{\mathrm{c}}(\omega) = e^{-j\omega T_0} \sum_{n=0}^{N-1} [(g_{n,1} - g_{n,3}) + j(g_{n,2} - g_{n,4})] e^{-j\omega T n} \tag{3}$$

where N is the number of c-taps, T_0 is the delay of the zero-th c-tap, T is the relative delay between two adjacent c-taps, and $g_{n,i}$ is the gain of the ith attenuator in c-tap n.

Note that since $g_{n,i}$ represent an attenuation value, then we have $0 \leq g_{n,i} \leq 1$ for all $n = 0, 1, ..., N-1$ and $i = 1, 2, 3, 4$. Therefore, $(g_{n,1} - g_{n,3}) + j(g_{n,2} - g_{n,4})$ can produce any complex value with real and imaginary parts within $[-1, 1]$ interval. The intuition behind the clustered architecture is that each c-tap can match a large number of clustered multipaths in the interference channel. And if T is chosen small enough, $\hat{H}_{\mathrm{c}}(\omega)$ can be tuned to match a wide range of the interference channel, provided that the delay spread of the interference channel is no larger than NT.

The choice of T depends on the bandwidth of interest W. Particularly, $T = \frac{r_T}{W}$ where $r_T < 1$. Simulation results has shown that $r_T = 0.1$ is a good choice and the performance is not sensitive to r_T when it is around 0.1. Note that a fixed delay is desirable since building programmable delays is extremely hard. The choice of N depends on the desired performance and the delay spread of the interference channel T_d. Theoretically, we need $NT \geq T_d$ to have a perfect interference cancellation if all multipaths are significant.

III. Tuning Algorithm

A. Ideal Attenuators

Here, we assume attenuators are ideal, i.e., (1) they do not introduce any phase-shift and (2) they can provide any attenuation value between 0 and 1 precisely.

For SIC, we need to match the cancellation channel to the interference channel in the bandwidth of interest. Let $f_1, \cdots, f_K$ be K sample frequencies that uniformly span the interval $[f_c - \frac{W}{2}, f_c + \frac{W}{2}]$ where f_c is the carrier frequency. Let $\mathbf{h} = [H(\omega_1), H(\omega_2), \cdots, H(\omega_K)]^T$ where $\omega_k = 2\pi f_k$ for all $k = 1, ..., K$. Also Let $\hat{\mathbf{h}} = [\hat{H}(\omega_1), \hat{H}(\omega_2), \cdots, \hat{H}(\omega_K)]^T$ where $\hat{H}(\omega)$ represents either $\hat{H}_c(\omega)$ or $\hat{H}_u(\omega)$. Let in the clustered architecture, $\boldsymbol{g} = [g_{n,i}]$, $\forall n = 0, 1, ..., N-1$, $\forall i = 1, 2, 3, 4$, a $4N \times 1$ vector, and in the uniform architecture, $\boldsymbol{g} = [g_n]$, $\forall n = 0, 1, ..., N-1$, a $N \times 1$ vector. Then for each architecture we can write $\hat{\mathbf{h}} = \mathbf{T}\boldsymbol{g}$ where based on equation (3) or (2), the matrix $\mathbf{T}$ is easy to construct.

For the clustered architecture (and similarly for the uniform architecture), to determine the optimal $\boldsymbol{g}$, we solve the following optimization problem:

$$\min_{0 \leq g_{n,i} \leq 1, \forall n, \forall i} \left\| \begin{bmatrix} Re\{\mathbf{h}\} \\ Im\{\mathbf{h}\} \end{bmatrix} - \begin{bmatrix} Re\{\mathbf{T}\} \\ Im\{\mathbf{T}\} \end{bmatrix} \boldsymbol{g} \right\| \tag{4}$$

where Re and Im stand for real and imaginary parts. The above constrained problem is a *convex optimization* which can be solved by the CVX software. Note that according to (3), solution to the optimization problem (4) is not unique.

B. Non-Ideal Attenuators

Here we assume attenuators are non-ideal. Particularly, two impairments introduced by attenuators are considered: phase-shift and quantization error. Let $g_{n,i} = r_{n,i} e^{j\theta_{n,i}}$ where $r_{n,i}$ and $\theta_{n,i}$ are the magnitude and phase-shift of attenuator $g_{n,i}$. In general, $\theta_{n,i}$ is a function of $r_{n,i}$, and to emphasize this fact, we rewrite $g_{n,i}$ as $g_{n,i} = r_{n,i} e^{j\theta_{n,i}(r_{n,i})}$.

Another impairment is quantization error introduced by digital-step attenuators. $r_{n,i}$ of each attenuator after quantization can only be such that $-20\log_{10} r_{n,i} \in \{0, \Delta, 2\Delta, ..., (2^{n_b}-1)\Delta\}$ where Δ is the step size and n_b is the number of control bits for the step attenuator. In other words, $r_{n,i}$ is quantized to $10^{-\frac{\Delta}{20}m_{n,i}}$ where $m_{n,i} = 0, 1, ..., 2^{n_b}-1$. Therefore, $r_{n,i}e^{j\theta_{n,i}(r_{n,i})}$ is quantized to $10^{-\frac{\Delta}{20}m_{n,i}}e^{j\theta_{n,i}(m_{n,i})}$.

Here, for the clustered architecture, to determine optimal $\boldsymbol{g}$, we solve the following optimization problem:

$$\min_{m_{n,i}=0,1,...,2^{n_b}-1, \forall n, \forall i} \sum_k |H(\omega_k) - \hat{H}(\omega_k, \boldsymbol{m})|^2 \quad (5)$$

where $\boldsymbol{m} = [m_{n,i}]$, $\forall n, \forall i$ is a $4N \times 1$ vector. The optimization problem (5) is an *integer optimization* and it can be solved by relaxation of integer constraints on decision variables, i.e., replacing the constraint with $0 \leq m_{n,i} \leq 2^{n_b}-1, \forall n, \forall i$, where $m_{n,i}$ is a real-valued variable. After solving the relaxed problem, each $m_{n,i}$ is rounded to the nearest integer. To solve the relaxed problem, the trust region reflective algorithm is used and the initial point for each $m_{n,i}$, is set to be $m_{\text{init}} = m_{\max} = 2^{n_b}-1$. Note that at this point, attenuation of attenuators are at their maximum possible level and the magnitude of $\hat{H}(\omega_k, \boldsymbol{m})$ is at its lowest value, and as a result, the objective function has a high value.

Note that phase errors of non-ideal power dividers can be incorporated into phase-shift of attenuators. Also amplitude reduction of the transmitted signal due to power dividers will be captured by attenuators.

IV. Performance Evaluation

To evaluate performance of the all-analog canceler, we define a relative power of the residual interference for the rth realization of the interference channel and the mth frequency (in dB) as follows:

$$e^{(r)}(\omega_k) = 10\log_{10} \frac{|\ H^{(r)}(\omega_k) - \hat{H}^{(r)}(\omega_k)\ |^2}{|\ H^{(r)}(\omega_k)\ |^2} \quad (6)$$

Also we define three averaged residuals: $E_1^{(r)} = \frac{1}{K}\sum_{k=1}^{K} e^{(r)}(\omega_k)$, $E_2(\omega_k) = \frac{1}{N_r}\sum_{r=1}^{N_r} e^{(r)}(\omega_k)$, $E_3 = \frac{1}{KN_r}\sum_{r=1}^{N_r}\sum_{k=1}^{K} e^{(r)}(\omega_k)$ where N_r is the number of realizations considered for the interference channel.

V. Simulation Results

In this section, the performance of the clustered and uniform architectures is compared. To have a fair comparison between two architectures, we choose $N_u = 4N_c$ and $T_u = \frac{T_c}{4}$ where N_c and N_u are the number of taps, and T_c and T_u are the relative delay between two adjacent taps in the clustered and uniform architectures orderly. This would cause that two cancelers have the same number of attenuators $4N_c = N_u$, and also the same delay spread $N_uT_u = N_cT_c$.

Simulation results are based on the following values of parameters: $T_0 = 0$, $f_c = 2.4$ GHz, $W = 100$ MHz, $K = 1000$, $T_c = \frac{0.1}{W}$, $N_c = 4$, $N_u = 16$, $T_u = \frac{0.1}{4W}$. For non-ideal attenuators, we set $s = -0.0276$ rad/dB, $\Delta = 0.01$ dB, and $n_b = 13$ bits. Each simulation is based on $N_r = 100$ random interference channels.

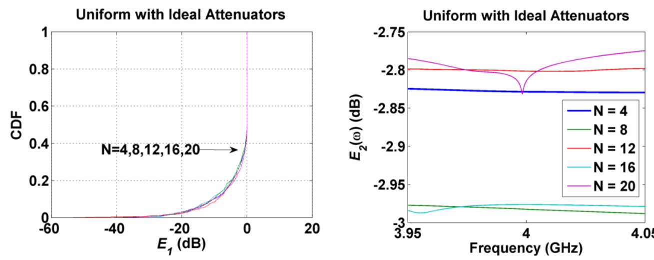

(a) CDF of E_1 (b) $E_2(\omega)$ vs. frequency

Fig. 2. Uniform canceler with ideal attenuators and an improper f_c ($f_c = 4GHz$).

A. Interference Channel Model

For statistical performance limits, the following random multipath interference channel model is used:

$$H(\omega) = \sum_{i=0}^{I-1} a_i e^{-j\omega\tau_i} \quad (7)$$

where I is the number of multipaths, τ_i is the delay of the ith multipath, and a_i is the amplitude of the ith multipath. To simulate a wide range of interference channels, it is assumed

$$a_i = \frac{\epsilon l_i d^{\alpha}}{(d + c\tau_i)^{\alpha}} \quad (8)$$

where l_i is a uniform random number within $(0,1)$, $d = 0.03$m, $c = 3\times10^8$m/s, τ_i is a uniform random number within $(0,1)\mu s$, and $\alpha \geq 1$ is the amplitude path loss exponent. We also choose $\tau_0 = 0$, $a_0 = \epsilon$, $I = 1000$ and $\epsilon = \frac{1}{1000}$. This choice of ϵ is to ensure that there is no effective gain in the interference channel since a canceler consisting of attenuators cannot provide a good cancellation in such a situation.

On the other hand, measurements of $H(\omega)$ is not perfect and the canceler uses noisy measurements $H_{noisy}(\omega)$ for tuning the attenuators rather than $H(\omega)$ where

$$H_{noisy}(\omega) = H(\omega) + w(\omega) \quad (9)$$

where $w(\omega)$ represents measurement noise. For each frequency, each of the real and imaginary parts of $w(\omega)$ is modeled as an independent uniform zero-mean random number. This noise results in an average SNR over the whole band $[f_c - \frac{W}{2}, f_c + \frac{W}{2}]$. In simulations, we set SNR=60dB.

B. Ideal Attenuators

Here, we investigate *limits* of the all-analog clustered and uniform cancelers. To do so, it is assumed perfect attenuators and no measurement noise ($w(\omega) = 0$). We also show that the performance of the clustered canceler is as good or better than the performance of the uniform canceler while the uniform canceler is also dependent to the choice of the carrier frequency.

Fig. 2 shows that performance of the uniform canceler is highly dependent to the choice of the carrier frequency and it can be completely ineffective if for a given T_u, f_c is not chosen properly (only 3dB cancellation). On the other hand, Fig. 3 shows the performance of the uniform canceler when a proper carrier frequency is chosen and the performance of the uniform canceler is at its best.

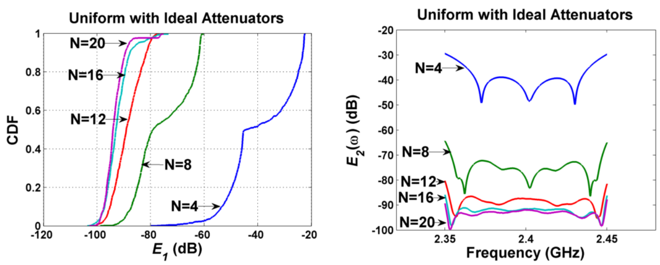

(a) CDF of E_1 (b) $E_2(\omega)$ vs. frequency

Fig. 3. Uniform canceler with ideal attenuators and a proper f_c ($f_c = 2.4GHz$).

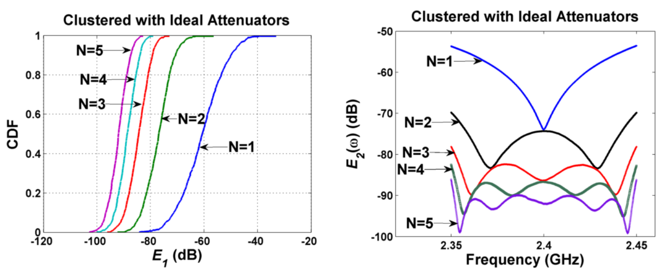

(a) CDF of E_1 (b) $E_2(\omega)$ vs. frequency

Fig. 4. Clustered canceler with ideal attenuators. $f_c = 2.4GHz$.

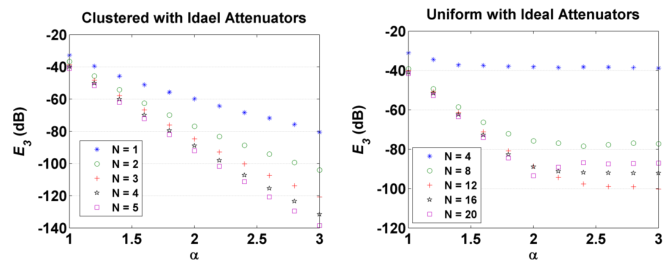

(a) Clustered Canceler (b) Uniform Canceler

Fig. 6. Impact of amplitude path loss exponent α on the performance of the cancelers with ideal attenuators for different values of N. $f_c = 2.4GHz$

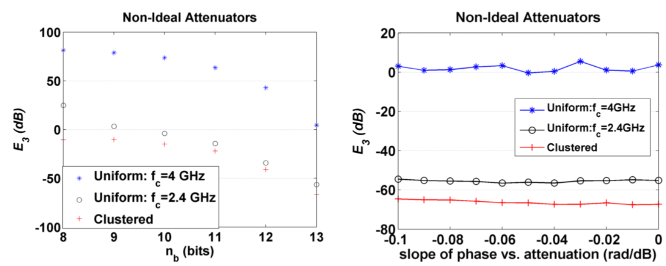

(a) Impact of n_b on performance. $N_c = 4, N_u = 16, \Delta = 0.01dB$.

(b) Impact of phase-shift of attenuators on performance. $N_c = 4, N_u = 16, \Delta = 0.01dB, n_b = 13$.

Fig. 7. Impact of n_b and phase-shift of attenuators on performance.

Fig. 4 shows that performance of the clustered canceler for $f_c = 2.4GHz$. Note that the clustered canceler is not dependent to the choice of the carrier frequency and the results for any other f_c would be the same (shown in Fig. 8).

Fig. 3(a) and 4(a) show that as the number of taps N increases, the residual interference decreases.

Fig. 3(b) and 4(b) show how the residual interference varies with frequency for different values of N. It can be seen that the residual interference is relatively high near the edges of the frequency band of interest.

Fig. 5 shows $r_T = 0.1$ is a good choice for $T = \frac{r_T}{W}$ and the performance is not sensitive to r_T when it is around 0.1. Also Fig. 5(b) shows that uniform canceler can be ineffective if for a given f_c, T_u is not chosen properly and $f_c T_u$ is equal to an integer. This is one of the advantages of the clustered canceler in compare to the uniform canceler.

Fig. 6 shows that performance is better in more obstructive environment (larger α). Fig. 6(a) shows that for the clustered canceler, the residual interference decreases linearly as the amplitude path loss exponent α increases.

Also our simulation shows the performance improves as the bandwidth of interest W decreases (not shown here).

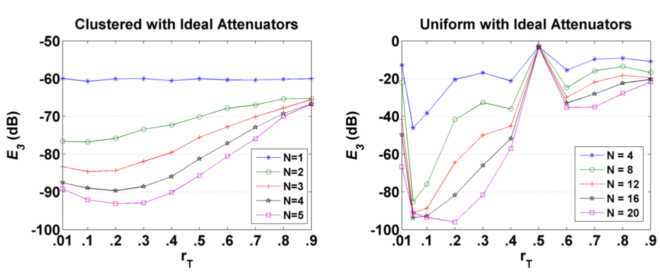

(a) Clustered Canceler (b) Uniform Canceler

Fig. 5. Impact of choice of $T_c = \frac{r_T}{W}$ and $T_u = \frac{r_T}{4W}$ on the performance of the cancelers with ideal attenuators for different values of N. $f_c = 2.4GHz$

C. Non-Ideal Attenuators

As mentioned in Section III-B, two impairments for non-ideal attenuators are considered, phase-shift and quantization error. Phase-shift introduced by an attenuator $\theta_{n,i}(r_{n,i})$ can be modeled as a linear function of attenuator magnitude $r_{n,i}$ in dB, i.e., $\theta_{n,i}(r_{n,i}) \propto -20\log_{10} r_{n,i}$ [6]. Therefore, $g_{n,i} = r_{n,i}e^{j\gamma \log_{10} r_{n,i}}$ where $\gamma_{n,i} = -20 s_{n,i}$ and $s_{n,i}$ is the slope of phase (in radian) vs. attenuation (in dB). For simulation, it is assumed $s_{n,i} = s, \forall n, \forall i$, and consequently, $\gamma_{n,i} = \gamma$. As a result, frequency response of the clustered canceler becomes

$$\hat{H}_c(\omega, \boldsymbol{r}) = \sum_{n=0}^{N-1} \Big[\left(r_{n,1}e^{j\gamma \log r_{n,1}} - r_{n,3}e^{j\gamma \log r_{n,3}} \right) + j \left(r_{n,2}e^{j\gamma \log r_{n,2}} - r_{n,4}e^{j\gamma \log r_{n,4}} \right) \Big] e^{-j\omega n T}$$

After quantization by digital-step attenuators, frequency response of the clustered canceler becomes

$$\hat{H}_c(\omega, \boldsymbol{m}) = \sum_{n=0}^{N-1} \left[\left(\eta^{m_{n,1}} - \eta^{m_{n,3}} \right) + j \left(\eta^{m_{n,2}} - \eta^{m_{n,4}} \right) \right] e^{-j\omega n T}$$

where $\eta = \left(10 e^{j\gamma}\right)^{-\frac{\Delta}{20}}$.

Fig. 7 shows impact of the parameters of non-ideal attenuators on the performance of the cancelers. As shown in Fig. 7(a) , as n_b increases, performance improves. However, the performance saturates when n_b is beyond a threshold for a given Δ (not shown here). This threshold depends on the value of Δ since the maximum attenuation is $(2^{n_b}-1)\Delta$dB. Fig. 7(b) shows impact of phase-shift of attenuators. As it can be seen, phase-shift does not have much impact on the performance.

D. Randomized Uniform

Here, we consider the case that the relative delay between two adjacent taps of the uniform structure, is not fixed. This

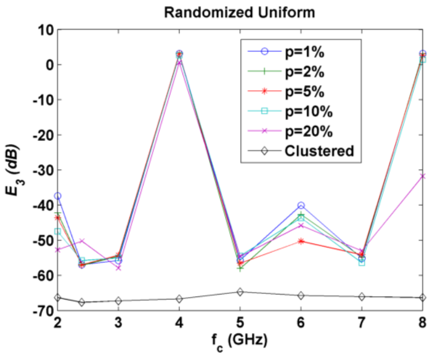

Fig. 8. Impact of perturbation in T_u on performance. $N_u = 16, \Delta = 0.01dB, n_b = 13$.

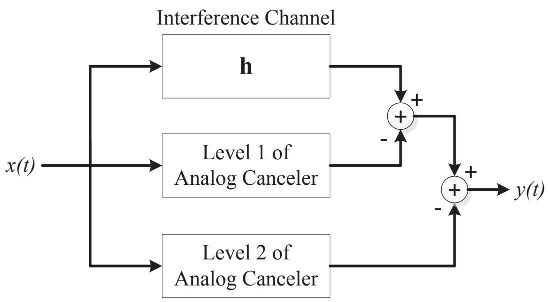

Fig. 9. System model for two-level all-analog canceler.

may be due to imperfect length of cables used to implement time delays. Particularly, in tap n, instead of having delay of nT, there is delay of $T_n = nT_u + \delta_n$, and as a result we have

$$\hat{H}_{\mathrm{r}}(\omega) = e^{-j\omega T_0} \sum_{n=0}^{N-1} g_n e^{-j\omega(nT_u+\delta_n)} \tag{10}$$

where $\delta_0 = 0$ and δ_n for $n = 1, ..., N-1$ are i.i.d. uniform random variables in $(-\delta_{max}, \delta_{max})$ and $\delta_{max} = T_u p$. For simulation, $p = 1\%, 2\%, 5\%, 10\%, 20\%$ is chosen.

Fig. 8 shows that in the uniform canceler for an improper carrier frequency, even changing T_u within 20% of T_u, does not improve the performance. It also shows that the clustered canceler is robust to the choice of the carrier frequency.

E. Multi-Level Cancellation

Structure of a general two-level canceler is shown in Fig. 9 where the residual of the first-level canceler is further reduced by the second level. Let the number of taps and relative delay between two adjacent taps in the first level be N_1 and T_1 and in the second level be N_2 and T_2. Here, we want to investigate if the multi-level canceler outperforms the single-level canceler where two cancelers have the same total number of taps and also the same delay spread. In other words, if the number of taps and the relative delay between two adjacent taps in the single-level canceler be N and T, such that $N = N_1 + N_2$ and $NT = \max\{N_1T_1, N_2T_2\}$, for a given interference channel which structure performs better. To evaluate the overall performance of multi-level canceler, the expression (6) is modified as follows:

$$e^{(r)}(\omega_k) = 10\log_{10} \frac{\mid H^{(r)}(\omega_k) - \hat{H}_1^{(r)}(\omega_k) - \hat{H}_2^{(r)}(\omega_k) \mid^2}{\mid H^{(r)}(\omega_k) \mid^2} \tag{11}$$

First, impact of two-level canceler on the clustered architecture is simulated and compared to the single-level clustered canceler. For the single-level with $N = 4$ and $T = \frac{0.1}{W}$, there is 67 dB cancellation, i.e., $E_3 = -67$ dB. For two-level canceler for $N_1 = 1$, $N_2 = 3$, $T_1 = \frac{0.1}{W}$, and $T_2 = \frac{NT}{N_2}$, there is 61 dB cancellation for the first level but 77 dB for the overall two-level cancellation. Interestingly, two-level clustered canceler outperforms the single-level clustered canceler.

Next, impact of two-level canceler on the uniform architecture is simulated and compared to the single-level uniform canceler. We assume a good carrier frequency for the uniform canceler ($f_c = 2.4GHz$). For the single-level with $N = 16$ and $T = \frac{0.1}{4W}$, there is 55 dB cancellation. For the two-level canceler for $N_1 = 4$, $N_2 = 12$, $T_1 = \frac{0.1}{4W}$, and $T_2 = \frac{NT}{N_2}$, there is 34 dB cancellation for the first level and 55 dB for the overall two-level cancellation. Interestingly, the two-level uniform canceler does not provide improvement over the single-level uniform canceler.

VI. Conclusion

We have proposed a novel architecture for an all-analog canceler. We have showed that in addition that the performance of the clustered canceler is as good or better than the uniform canceler, its performance is also independent of the carrier frequency. We have also provided a statistical evaluation of the performance of both all-analog cancelers for ideal and non-ideal attenuators. We believe that this work is important for guiding expectations of results and the implementation of more ambitious and thorough hardware-based experiments.

References

[1] Y. Hua, Y. Ma, P. Liang, and A. Cirik, "Breaking the barrier of transmission noise in full-duplex radio," in *MILCOM 2013*.

[2] J. I. Choi, M. Jain, K. Srinivasan, P. Levis, and S. Katti, "Achieving single channel, full duplex wireless communication," in *Proceedings of the sixteenth annual international conference on Mobile computing and networking*. ACM, 2010, pp. 1–12.

[3] S. S. Hong, J. Mehlman, and S. Katti, "Picasso: flexible rf and spectrum slicing," *ACM SIGCOMM Computer Communication Review*, vol. 42, no. 4, pp. 37–48, 2012.

[4] J. G. McMichael and K. E. Kolodziej, "Optimal tuning of analog self-interference cancellers for full-duplex wireless communication," in *Communication, Control, and Computing (Allerton), 2012 50th Annual Allerton Conference on*. IEEE, 2012, pp. 246–251.

[5] D. Bharadia, E. McMilin, and S. Katti, "Full duplex radios," in *Proceedings of the ACM SIGCOMM 2013 conference on SIGCOMM*. ACM, 2013, pp. 375–386.

[6] Y. Choi and H. Shirani-Mehr, "Simultaneous transmission and reception: Algorithm, design and system level performance," *IEEE Transactions on Wireless Communications, to appear*.

[7] M. A. Khojastepour and S. Rangarajan, "Wideband digital cancellation for full-duplex communications," in *Signals, Systems and Computers (ASILOMAR), 2012 Conference Record of the Forty Sixth Asilomar Conference on*. IEEE, 2012, pp. 1300–1304.

[8] M. Duarte and A. Sabharwal, "Full-duplex wireless communications using off-the-shelf radios: Feasibility and first results," in *Signals, Systems and Computers (ASILOMAR), 2010 Conference Record of the Forty Fourth Asilomar Conference on*. IEEE, 2010, pp. 1558–1562.

[9] A. Sahai, G. Patel, and A. Sabharwal, "Pushing the limits of full-duplex: Design and real-time implementation," 2011.

[10] Y. Hua, P. Liang, Y. Ma, A. C. Cirik, and Q. Gao, "A method for broadband full-duplex mimo radio," *Signal Processing Letters, IEEE*, vol. 19, no. 12, pp. 793–796, 2012.